

Some aerodynamic features of a cotton canopy

By D. H. BACHE* and M. H. UNSWORTH

Nottingham University, School of Agriculture, Department of Physiology and Environmental Studies, Sutton Bonington, Loughborough, Leicestershire, U.K.

(Received 13 May 1975; revised 2 June 1976)

SUMMARY

Analysis of profiles measured over irrigated cotton in the Sudan Gezira showed that the crop boundary layer remained stable throughout most of the day. The shape of wind profiles measured within the canopy suggested that momentum was absorbed mostly in the upper layers of the canopy, with the lower regions remaining isolated from the microclimate above. A similarity analysis based on dynamic scaling factors yielded a generalized wind profile from which momentum diffusivities and mixing lengths were calculated. The analysis showed that aerodynamic features of the upper layers of the canopy were characterized by the friction velocity and the height of the zero-plane displacement.

1. INTRODUCTION

A better understanding of the turbulent transfer processes within and above crop canopies depends on providing an accurate description of canopy aerodynamics. This is not a simple task since aerodynamic features, linked with canopy structure and temperature gradients, reflect many aspects of crop physiology and crop environment. For adiabatic flow much useful progress has been made toward rationalizing crop aerodynamics in studies by Inoue (1963), Cionco (1965), Isobe (1964), Cowan (1968) and Thom (1971).

In a recent review of cotton and its environment, Stanhill (1976) noted that much less was known about wind flow within the canopy than about other aspects of its microclimate, e.g. Davenport and Hudson (1967), Rijks (1968), Stanhill and Fuchs (1968). The present studies, related to crop spraying (Bache 1975), were conducted in the Gezira region of Sudan and concerned the Barakat variety, *Gossypium barbadense*, of cotton. The broad features of canopy aerodynamics are emphasized rather than the characteristics of individual elements.

(a) *The Gezira; aspects of climate*

The Gezira irrigation scheme, adjoining the Blue Nile and centred on 14°N 33°E, is situated on a plain with average slope 0.02% to the north. It covers an area of one million hectares, of which 40-45% is normally under crop. General features of the scheme were described by Allan and Smith (1948), and the climate was described by Ireland (1948), and Thompson (1965).

An important feature of the climate during the period of measurement (7 October to 5 November 1973) was the relatively sudden change in wind direction from southerly to northerly in late October, due to the southern movement of the intertropical convergence. The hot, dry and dusty air in the northerly winds influences the short and long wave radiation budgets (Rijks 1968) and during the ensuing months, crops in the Gezira are subject to considerable large scale and local advection of heat (Davenport and Hudson 1967). Windspeeds from the north are generally greater than from the south. The windspeed usually has a

* Now at the University of Strathclyde, Civil Engineering Department, Colville Building, 48 North Portland Street, Glasgow G1 1XN.

relatively strong peak around mid-morning and a weaker peak during the late afternoon, related to diurnal pressure variation (Geiger 1965).

2. EXPERIMENTAL

Instruments were placed centrally in an irrigated cotton field surrounded by unirrigated fallow; the fetch over cotton varied between 130 m and 500 m. Profiles of mean windspeed and temperature gradient were measured within and above the cotton canopy and a simplified analysis of crop structure was attempted to interpret 'in canopy' airflow.

(a) Windspeed measurement

(i) *Above-canopy.* Windspeeds above the crop were measured using six miniature cup anemometers (Rimco, CSIRO) mounted on a mast with the top anemometer 4.8 m above the ground and the bottom anemometer approximately 0.1 m above the crop. The anemometers were calibrated against a standard cup anemometer in a wind tunnel at speeds of 0.7–7.0 m s⁻¹. In non-turbulent flow windspeeds were accurate to within 1%. Wind profiles were generally based on an averaging time of 24 min.

(ii) *Within-canopy.* Within the crop, windspeeds were measured at five levels using sets of heated thermocouple anemometers (Baines 1968). A further set of anemometers was positioned at the level of the lowest cup anemometer. Small corrections for drift in heater current were determined from comparison of cup and thermocouple anemometers at this level. Each set consisted of four sensors spaced horizontally at 0.15 m intervals, with heater input and voltage outputs linked in series. The output signal from each level was integrated over four 30 s periods equally spaced over a total sampling time of 24 min. Probes, calibrated in streamline flow in a wind tunnel, had a working range of 0.05–4.00 m s⁻¹. Inspection of results suggests that, within the canopy, windspeed could usually be assessed to within 0.05 m s⁻¹.

(b) Temperature measurement

Temperature measurements were necessary for evaluating the effects of stability. Because of the remoteness of the experimental site, a portable and easily maintained temperature measurement system was used.

Temperature differences were measured at eight levels, four within the crop and four above the crop using fine wire thermocouples.

A mast was constructed to support a single vertical constantan wire (0.155 mm diameter) with copper wires of similar dimension soldered to it to form thermocouple junctions. Using the top junction as a reference level, the voltage between it and any other level could be selected with a manual switching unit. The measured output signal from any individual level was amplified and integrated. The integrator sent pulses to a mechanical counter at a rate proportional to the temperature difference measured.

Temperature differences between each level and the top thermocouple were sampled sequentially for periods of 45 s: 30 s for integration and 15 s for switching, etc. The cycle of sampling all levels (including a zero check) took 6 min and the process was repeated to build up a mean profile over 24 min. Using this procedure, gradients could be measured to within 0.03 degC/m on the most sensitive amplification range. Radiation errors, typically 0.03 degC, did not influence stability corrections.

Inspection of data showed that additional errors were introduced when measuring profiles under non-steady conditions. At dawn, when the above-crop temperature gradient

was changing most rapidly ($\sim 1 \text{ degC m}^{-1} \text{ h}^{-1}$), the error in the mean gradient between consecutive measurements (45 s apart) was 0.01 degC m^{-1} . This over the total sampling period leads to a maximum systematic error of 0.04 degC m^{-1} .

Examples of some wind profiles at high and low windspeeds are shown in Fig. 1. An example of the daily trend in temperature distribution is shown in Fig. 2.

3. ANALYSIS

(a) Crop characteristics

During the period of measurement, the average crop height increased from 1.0 to 1.46 m with a maximum height variation of $\pm 0.2 \text{ m}$. Foliage distribution was analysed as described in Bache and Uk (1975). A stratified clip showed that within the upper 0.6 m of the canopy, foliage density was evenly distributed with height. Over the observed period of growth, the leaf area index increased from approximately 4.5 to 6.5. Further detail of growth and structure is given in Munro and Farbrother (1969).

(b) Aerodynamic crop height

For this analysis, the canopy height h is defined in aerodynamic terms as the height of the point of inflexion (see Fig. 1) between the 'in-canopy' and 'above-canopy' wind profiles. The value of h was generally within 15 cm of the average crop height. Using this reference level considerably reduced the amount of scatter in subsequent analysis.

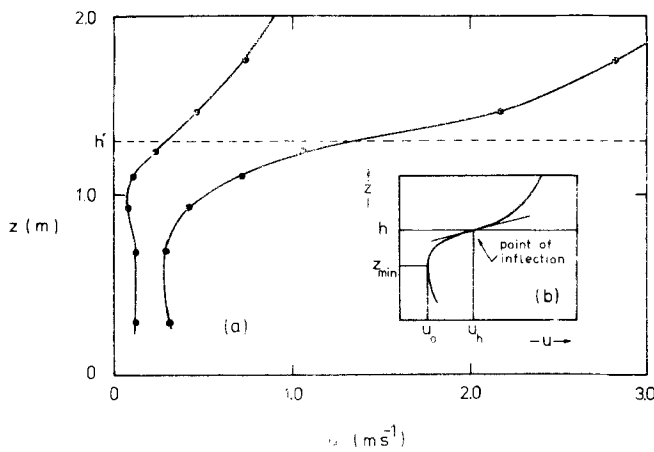


Figure 1. (a) Examples of the variation of windspeed u with height z above the ground at high and low windspeed. h' is the approximate crop height. (b) A schematic wind profile defining the aerodynamic crop height h at a point of inflexion and the coordinates z_{\min} and u_0 at a turning point.

(c) Characteristics above the crop

With stable conditions prevailing throughout most of the day, the majority of profiles above the crop were analysed using the log-linear profile (Webb 1970)

$$u = (u_* / k) \{ \ln[(z - d) / z_0] - (\alpha / L)(z - d - z_0) \} \quad (1)$$

where u is the windspeed at height z , u_* the friction velocity, d the zero-plane displacement, z_0 the roughness length, L the Obukhov length, α the Monin-Obukhov coefficient (taken as 5.2) and k von Kármán's constant (taken as 0.40).

The zero-plane displacement was found by choosing an initial value, calculating an

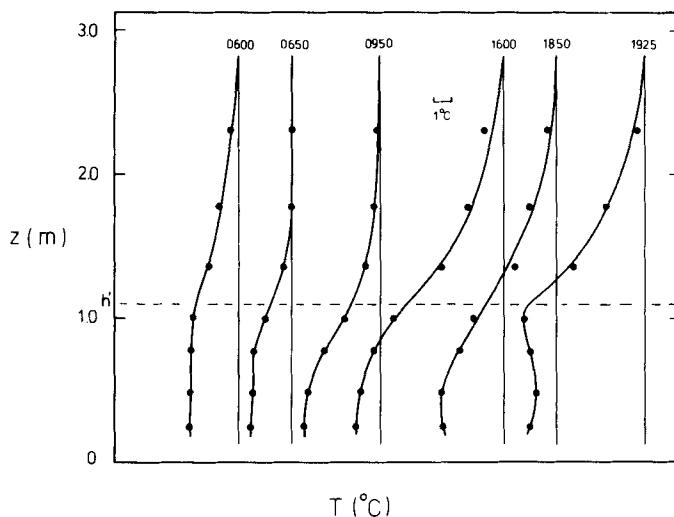


Figure 2. A typical variation of temperature with height z above the ground at different times of the day. h is the approximate crop height.

estimate of L from wind and temperature gradients and examining the curvature of a graph of u against $\{\ln(z-d) - \alpha(z-d-z_0)/L\}$. An initial estimate of z_0 was made from Thom's (1971) expression for a bean crop: $z_0 = 0.36(h-d)$. The optimum value of d , corresponding to least curvature, was found and then the slope and intercept of the graph gave u_* and z_0 .

Figs. 3 and 4 show the variation of d/h and z_0/h with u_* and with the interface Richardson number $Ri(h)$.^{*} For near-neutral conditions, $|Ri(h)| < 0.01$, d/h and z_0/h vary as discussed by Monteith (1973). The trend shown in Fig. 3 represents a join of the average values

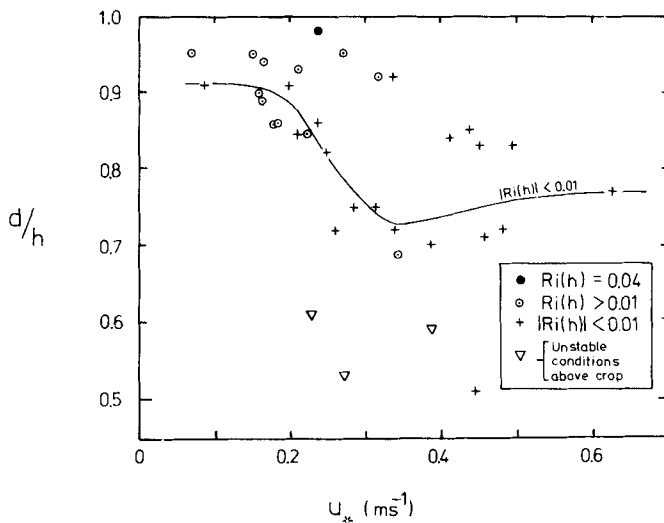


Figure 3. Variation of d/h with friction velocity u_* and stability. d is the zero-plane displacement and h the aerodynamic crop height (Fig. 1). Stability classes are represented by the interface Richardson number $Ri(h)$.

^{*} Calculations of L were based on an approximated Richardson number $Ri = g(dT/dz)/(T(du/dz)^2)$ which neglects the buoyancy forces arising from the water vapour flux. Order of magnitude calculations based on a likely humidity gradient ($\sim 1 \text{ mb m}^{-1}$) over cotton (Rijks 1971) show that the true Richardson number is underestimated by approximately 0.005 at average windspeed ($u_* \sim 0.25 \text{ m s}^{-1}$) and by approximately 0.05 in the most stable conditions (generally with $u_* \leq 0.1 \text{ m s}^{-1}$). Errors in Ri influence the authors' evaluation of d . Sample calculations indicate that d is overestimated by 1% in average conditions and by approximately 5% in very stable conditions.

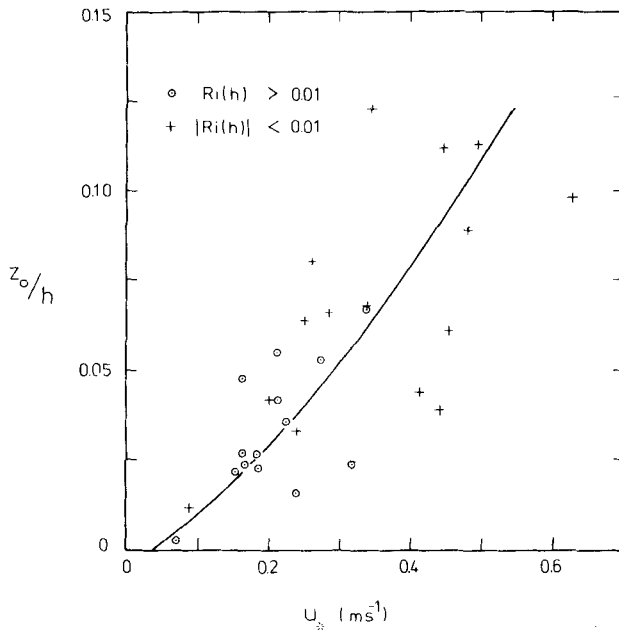


Figure 4. Variation of z_0/h with friction velocity u_* and stability. z_0 is the roughness length and h the aerodynamic crop height (Fig. 1). Stability classes are represented by the interface Richardson number $Ri(h)$.

of d/h in the intervals of $0.2 < u_* \leq 0.3$, $0.3 < u_* \leq 0.4 \text{ m s}^{-1}$ etc. Averaging the values independent of u_* yields $d/h = 0.79 \pm 0.10$ for $|Ri(h)| < 0.01$ which compares with $\overline{d/h} = 0.89 \pm 0.08$ for $Ri(h) > 0.01$ and 0.58 ± 0.04 for unstable conditions above the crop. The effect of stability on the penetration of the wind into the canopy is evident; relatively little penetration occurs in very stable conditions and at low windspeeds, but enhanced penetration occurs in unstable conditions. Values of d/h are generally larger than those reviewed by Stanhill and Fuchs (1968) and Stanhill (1975), probably because this crop had a large foliage density.

(i) *Variations in boundary layer stability.* Fig. 5 shows the typical trend of stability during days in the middle of the irrigation cycle when the soil was relatively dry. At sunrise, the night-time inversion was quickly destroyed and conditions were temporarily unstable between 0645 and 0830h. Thereafter, stability increased gradually throughout the day and

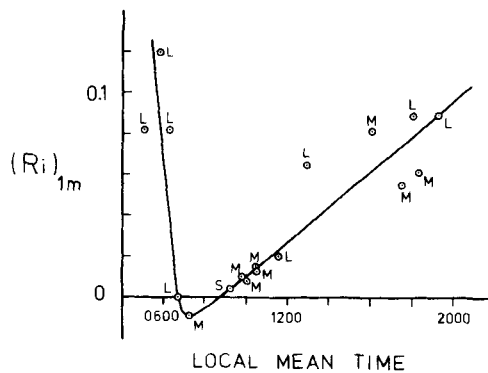


Figure 5. Hourly trend in stability over a cotton field in relatively dry conditions. The degree of stability is represented by a reference Richardson number $(Ri)_{1m}$, calculated from measured wind and temperature profiles at 1 m above the zero-plane displacement level. Windspeed categories are represented by the symbols L, M, S corresponding to low ($< 1.5 \text{ m s}^{-1}$), medium ($1.5\text{--}3.0 \text{ m s}^{-1}$) and strong ($> 3 \text{ m s}^{-1}$) winds.

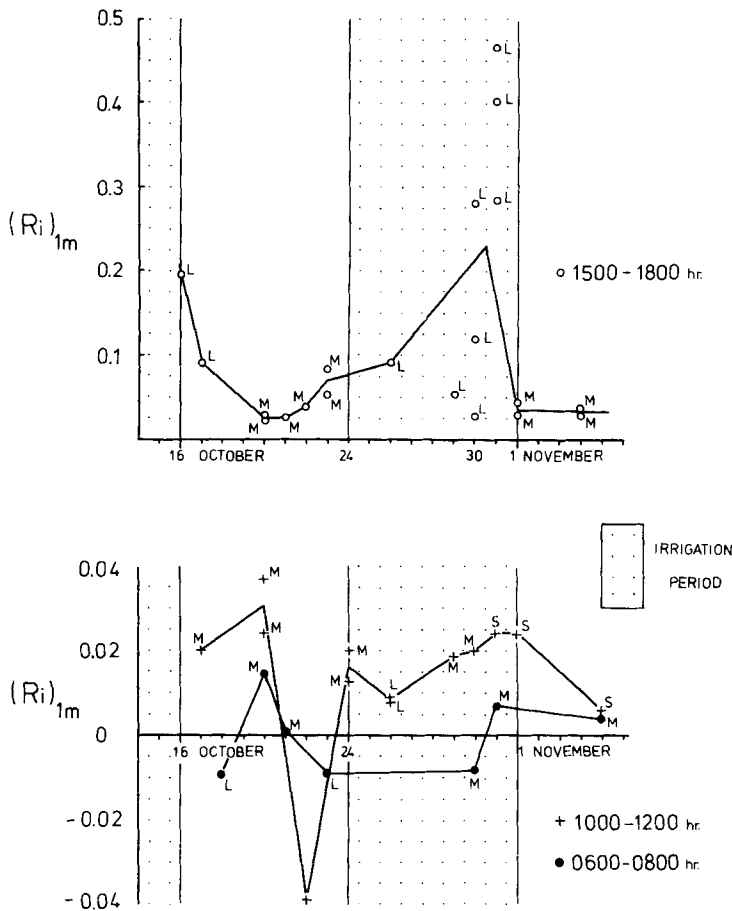


Figure 6. Trends in stability during the course of the irrigation cycle at selected periods during the day. The degree of stability is represented by a reference Richardson number $(Ri)_{1m}$ taken at 1 m above the zero-plane displacement. Windspeed categories are as defined in Fig. 5. Components of two irrigation periods appear, the first ending 16 October and the second taking place between 24 October and 2 November.

very stable conditions prevailed by sunset. Windspeed categories included in Fig. 5 show that light winds were associated with very stable conditions, particularly at dawn and in the afternoon and evening. When the soil was drier, the unstable period extended into the early afternoon.

The degree of stability depended on the stage in the irrigation cycle, particularly during the late afternoon when stable conditions were generally well developed. Fig. 6 illustrates this behaviour and shows that strongly stable conditions occurred toward the end of the second irrigation period. In the morning, however, conditions were never far from neutral.

(d) Windspeed within the canopy

(i) *Canopy partition.* With few exceptions, internal wind profiles followed the general shape seen in Fig. 1(a) and shown schematically in Fig. 1(b). The profile shape shows two regimes of behaviour: an upper region with $z_{min} \leq z \leq h$ where most of the momentum was absorbed; and a lower region, $z < z_{min}$, which appeared to be virtually isolated from airflow above.

(ii) *Aerodynamic features of the lower canopy.* The interpretation of windspeeds in the

lower canopy ($z < z_{\min}$) is difficult since observed changes in windspeed were of the same order as the experimental error. The general variation of windspeed followed the behaviour of u_0 (discussed later) and it was evident that, as the crop grew denser, the lower canopy microclimate became increasingly isolated from the microclimate above. Gradients of windspeed, $|du/dz|$, averaged between $z = 0.2$ m and z_{\min} , showed consistent increases whenever the atmosphere in the lower canopy became unstable; this often occurred around dusk (see Fig. 2).

(iii) *Aerodynamics of the upper canopy.* Airflow within the upper part of the canopy is generally represented, e.g. Inoue (1963), Thom (1971), by the one-dimensional vertical transfer equations

$$d\tau/dz = \rho c_D a(z) u^2(z) \quad . \quad . \quad . \quad (2)$$

$$\tau = \rho l^2 (du/dz)^2 \quad . \quad . \quad . \quad (3)$$

$$K_m = l^2 du/dz \quad . \quad . \quad . \quad (4)$$

where $d\tau/dz$ is the stress divergence, $u(z)$ is the windspeed at height z , ρ is air density, c_D is the drag coefficient of plant elements with effective aerodynamic surface area of vegetation $a(z)$ per unit volume, l is a mixing length and K_m the diffusivity of momentum. Combination of Eqs. (2)–(4) leads to

$$K_m(z) = \{\tau(h) - \int_z^h \rho c_D a u^2 dz\} / \{\rho (du/dz)_z\} \quad . \quad . \quad (5)$$

This scheme of analysis has been successful for predicting momentum transfer in the upper canopy, but fails in the domain $du/dz \leq 0$. It suggests that vertical transfer must be treated on a two-dimensional basis with the inclusion of pressure gradient terms as discussed in Bergen (1975) and by Businger (1975). A consideration of the equations involved, e.g. Bergen, shows that these are not easily resolved without comprehensive experimental data.

A key problem is the representation of the effective drag exerted by foliar elements. It has been found, e.g. Thom (1971), that the effective drag of an element within a canopy is less than the value when measured in isolation. This feature led Thom and others to introduce a shelter factor which allows for the behavioural difference. An alternative scheme was developed by Bergen, who derived the transfer equations in terms of an effective porosity; this takes account of the fraction of space occupied by the flow which contributes to the large-scale mass flux.

Another approach, which helps circumvent the problem of the turning point in the wind profile, is to make the working hypothesis that $d\tau/dz \neq 0$ when $du/dz = 0$.

To satisfy the hypothesis, the measured velocity is interpreted as comprising two components; first, an effective drag-velocity u_e (for inclusion in Eq. (2)) and second, a component u_0 defined so that $u_e = 0$ at $z = z_{\min}$. A feasible choice of u_e is

$$u_e = u - u_0 \quad . \quad . \quad . \quad (6)$$

where u is the measured windspeed, taking value u_0 at $z = z_{\min}$. Although the choice of Eq. (6) is somewhat arbitrary, it represents a simple approximation and recognizes several features which cannot easily be specified.

First, it should be noted that not all the measured velocity contributes to stress divergence as represented by Eq. (2). den Hartog and Shaw (1975) calculated leaf drag by defining the effective velocity as the mean value of the total instantaneous velocity resolved in the direction of the mean wind. Their approach breaks away from the usual approach of defining drag characteristics in terms of the mean flow. It may be valid for low-frequency turbulent components, but is unlikely to be an accurate description for the high-frequency components, since these are likely to interact with the fluctuations associated with the boundary layer

pressure fields of the foliar elements. The approach also lacks discrimination between motion whose energy is derived through vertical transfer, and motions resulting from thermal instabilities. Evidence (discussed later) suggests that thermally-driven windspeed may attain 0.1 m s^{-1} within a cotton canopy. The measured windspeed also includes a small contribution ($\sim 0.02 \text{ m s}^{-1}$) arising from the synoptic pressure gradient; again this contributes to u_0 . A second feature recognized by Eq. (6) is that any drift in the anemometer heater current manifests itself as a shift in the origin of the velocity coordinate. Third, it should be noted that Eq. (6) modifies only the integrated drag term leaving the magnitude of velocity gradient unaltered.

With this scheme, a dimensionless height Z can be defined by

$$Z = (z - z_{\min}) / (h - z_{\min}) \quad . \quad . \quad . \quad (7)$$

and a dimensionless velocity U by

$$U = (u - u_0) / (u_h - u_0) \quad . \quad . \quad . \quad (8)$$

where u_h is the velocity at $z = h$.

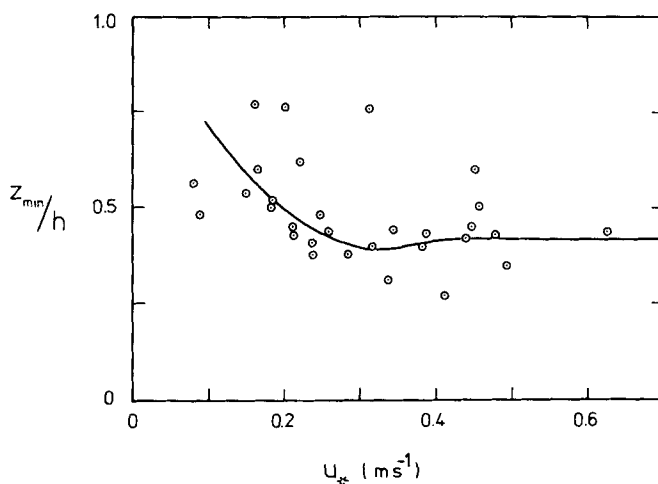


Figure 7. Variation of the ratio z_{\min}/h with friction velocity u_* . z_{\min} is the height of a turning point in the in-canopy wind profile and h the aerodynamic crop height (Fig. 1).

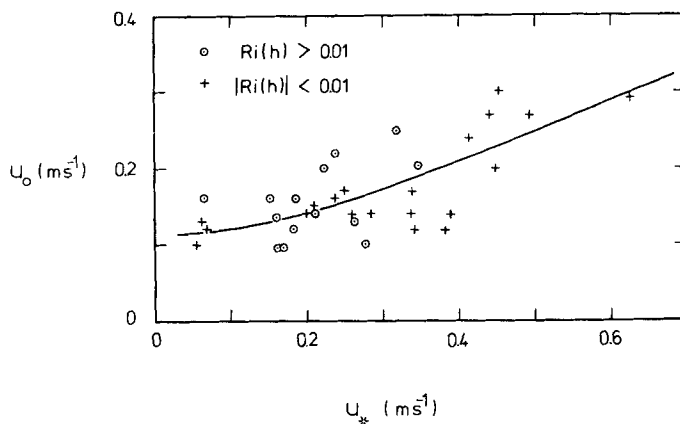


Figure 8. Variation of the velocity minimum u_0 with friction velocity u_* . u_0 is the velocity at the turning point in the in-canopy wind profile (Fig. 1). Stability categories are represented by the interface Richardson number $Ri(h)$ where h is the aerodynamic crop height (Fig. 1).

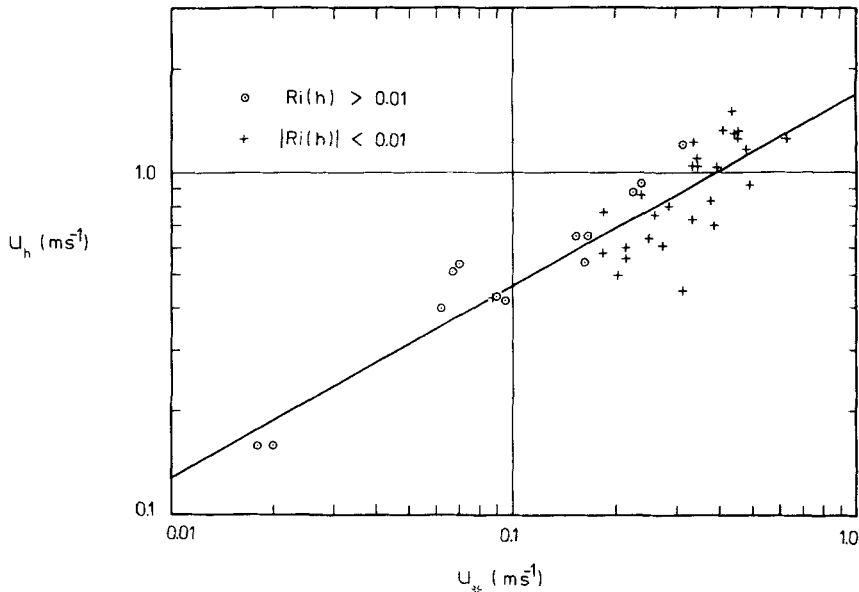


Figure 9. Variation of the windspeed u_h (Fig. 1) with the friction velocity u_* . Stability categories are represented by the interface Richardson number $Ri(h)$ where h is the aerodynamic crop height (Fig. 1).

The responses of z_{\min} , u_0 and u_h to external conditions are shown in Figs. 7–9. Fig. 7 shows that z_{\min}/h behaves in much the same way as d/h (Fig. 3) to changes in u_* (i.e. decreases with increasing u_*), though the response to interface stability is not consistent. Figs. 3 and 7 both show that as u_* increases, the depth of penetration of wind into the canopy increases at first, but with u_* exceeding 0.3 m/s, further penetration becomes difficult. However, Fig. 8 shows that u_0 increases systematically with u_* . Of interest is the extrapolated value $u_0 \sim 0.12 \text{ m s}^{-1}$ at $u_* = 0 \text{ m s}^{-1}$. The magnitude of u_0 cannot be explained by experimental error. If $u_* = 0 \text{ m s}^{-1}$ is interpreted as absence of mechanical stirring, it suggests that the air movements have derived their energy from thermal instabilities. This view is consistent with the stability behaviour noted in section 3(d)(ii). A similar feature was observed by Oliver (1975) within a forest canopy. In Fig. 9 the relationship between u_h and u_* is fairly well fitted by the relationship $u_h = Au_*^n$, with $A = 1.69 \pm 0.12$ and $n = 0.56 \pm 0.04$, which indicates that u_h becomes gradually less sensitive ($n < 1$) to increase in u_* . This suggests that mechanical energy is being dissipated over a greater depth of the canopy as windspeeds increase – again illustrating the penetration behaviour seen in Figs. 3 and 7.

(e) *A generalized wind profile*

Fig. 10 shows 28 wind profiles measured throughout the period of observation, with u_* in the range 0.07 to 0.63 m/s. Velocities and corresponding heights were scaled using Eqs. (7) and (8). The points correspond to windspeeds read off at 0.1 m intervals in the region $z_{\min} \leq z \leq h$ from smoothed curves through the original measured values. This procedure was adopted to isolate variations in profile shape, and it introduced only minor distortions in the discrete gradients existing between adjacent measured points. Subsequent analysis showed that over four weeks of observation, the average scaled profile was independent of crop height and was insensitive to Richardson numbers at h . Fig. 10 shows that, to a good approximation, windspeed was a unique function of Z , i.e. $U = \phi(Z)$, which for convenience is referred to as the ‘generalized’ velocity profile. Several authors, Inoue (1963), Saito (1964), Uchijima and Wright (1964), have found that the variation of wind speed within crops may

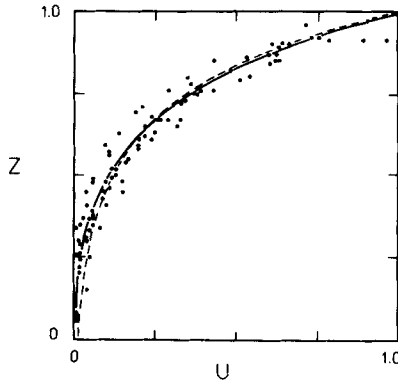


Figure 10. A generalized wind profile within the upper layers of the canopy based on 28 measured profiles. The coordinates Z and U represent a dimensionless height defined by $Z = (z - z_{min}) / (h - z_{min})$ and a dimensionless velocity $U = (u - u_0) / (u_h - u_0)$ with parameters z, z_{min}, h, u_0, u_h as defined in Fig. 1. The solid line is the line of best fit and the dashed line an exponential fit $U = \exp(-4.3(1-Z))$.

be represented by an exponential function of height. The relationship $U = \exp(-B(1-Z))$, plotted in Fig. 10 with $B = 4.3$, fits the measurements fairly well.

(f) *Eddy diffusivity for momentum*

Recognizing the uniformity of foliage density in the upper canopy and assuming that the drag coefficient was independent of windspeed and therefore of height within this region (Wright and Brown 1967; den Hartog and Shaw 1975), Eqs. (2)–(4) and (6) lead to

$$K_m(z) = (c_D a \int_{z_{min}}^z u_e^2 dz) / (du_e/dz)_z \quad (9)$$

Application of the boundary conditions $\tau = \rho u_*^2$ at $z = h$ and $\tau = 0$ at $z = z_{min}$ gives

$$c_D = u_*^2 / (a \int_{z_{min}}^h u_e^2 dz) \quad (10)$$

Combining Eqs. (9) and (10) and writing them in dimensionless form using Eqs. (7) and (8) yields

$$K_m(z) = \frac{u_*^2 h - z_{min} \int_0^z U^2 dZ}{\beta^2 u_h - u_0 |dU/dZ|_z} \quad (11)$$

where $\beta^2 = \int_0^1 U^2 dZ$. From Eq. (11) the shape of the diffusivity profile can be conveniently expressed by taking the ratio

$$\frac{K_m(z)}{K_m(h)} = \frac{\int_0^z U^2 dZ |dU/dZ|}{\int_0^1 U^2 dZ |dU/dZ|} \quad (12)$$

which is shown in Fig. 11. Fig. 11 shows that Eq. (12) is well represented by the exponential form

$$K_m(z) = K_m(h) \exp\{-C(1-Z)\} \quad (13)$$

with $C = 5.5$.

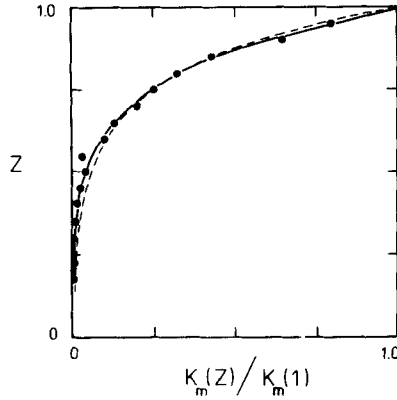


Figure 11. A dimensionless diffusivity profile calculated from the generalized wind profile (Fig. 10) using Eq. (12) $K_m(Z)$ is the momentum diffusivity at dimensionless height Z as defined in Fig. 10 and $K_m(1)$ the corresponding diffusivity at the interface. The solid line is a line of best fit and the dashed line an exponential fit $K_m(Z)/K_m(1) = \exp(-5.5(1-Z))$.

To examine the behaviour of the interface diffusivity, $K_m(h)$, it is useful to write Eq. (11) in the form

$$\frac{K_m(h)}{u_* (h-d)} = \frac{\Psi}{|dU/dZ|_1} \quad (14)$$

where

$$\Psi = \left(\frac{u_*}{u_h - u_0} \right) \left(\frac{h - z_{min}}{h - d} \right) \quad (15)$$

In Eq. (14) the denominator representing the slope of the generalized wind profile at $Z = 1$ is (from Fig. 10)

$$|dU/dZ|_1 = 3.5 \pm 0.50 \quad (16)$$

In Eq. (15) Ψ contains terms which depend on u_* and stability (see Figs. 3, 7, 8). Fig. 12

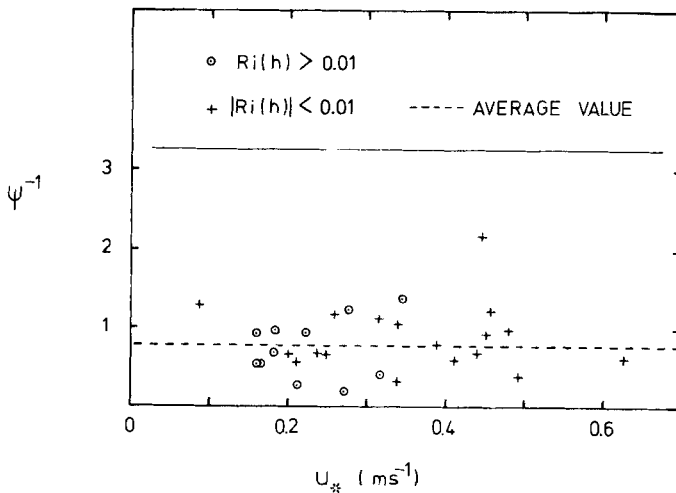


Figure 12. Variation of the parameter $\Psi = u_* (h - z_{min}) / ((u_h - u_0) (h - d))$ with friction velocity u_* and interface Richardson number $Ri(h)$. Parameters h, z_{min}, u_h, u_0 , are as defined in Fig. 1 and d is the zero-plane displacement. The dashed line refers to Ψ^{-1} which is seen to be independent of $Ri(h)$.

shows*, however, that within the limits of experimental scatter, Ψ^{-1} does not correlate with u_* or stability. Estimates of Ψ for any u_* can be obtained using the average value $\overline{\Psi^{-1}}$. Excluding the point $\Psi^{-1} > 2$ (Fig. 12) the data yield

$$\overline{\Psi^{-1}} = 0.78 \pm 0.32 \quad . \quad . \quad . \quad (17)$$

Combining Eqs. (14), (16) and (17) gives

$$K_m(h)/u_*(h-d) = 0.37 \pm 0.16. \quad . \quad . \quad . \quad (18)$$

It is common practice to assume that

$$K_m(h) = ku_*(h-d) \quad . \quad . \quad . \quad (19)$$

and it is seen, within the limits of experimental error, that Eq. (18) is consistent with that assumption.

(g) *Momentum mixing length*

From the basic definition the momentum mixing-length may be written

$$l^2 = \frac{K_m(z)}{\left| \frac{du}{dz} \right|_z} = \frac{K_m(z)/K_m(h)}{\left| \frac{du}{dz} \right|_z} \frac{K_m(h)}{\left| \frac{du}{dz} \right|_h} \quad . \quad . \quad . \quad (20)$$

Writing the gradient terms in dimensionless form

$$\left| \frac{du}{dz} \right|_z / \left| \frac{du}{dz} \right|_h = \left| \frac{dU}{dZ} \right|_z / \left| \frac{dU}{dZ} \right|_1 \quad . \quad . \quad . \quad (21)$$

and noting that

$$\frac{K_m(h)}{\left| du/dz \right|_h} = \frac{K_m^2(h)}{u_*^2} = k^2(h-d)^2 \quad . \quad . \quad . \quad (22)$$

leads to

$$l/\{k(h-d)\} = f(Z) \quad . \quad . \quad . \quad (23)$$

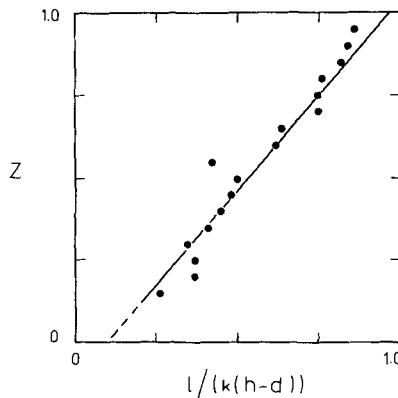


Figure 13. The variation of the mixing length ratio $l/k(h-d)$ with dimensionless height Z as defined in Fig. 10. l is the momentum mixing length calculated from Eqs. (23), (24) using the generalized wind profile (Fig. 10) and the momentum diffusivity profile (Fig. 11). k is von Kármán's constant (taken as 0.40), h is the aerodynamic crop height (Fig. 1) and d the zero-plane displacement.

* Large values of Ψ occur when $h-d$ is small and Ψ is sensitive to this difference. To minimize the apparent influence of errors in $h-d$, Fig. 12 has been drawn to show Ψ^{-1} against u_* .

where

$$(Z) = \left[\frac{K_m(Z)/K_m(1)}{\left| \frac{dU}{dZ} \right|_z / \left| \frac{dU}{dZ} \right|_1} \right]^{\frac{1}{2}} \quad (24)$$

Fig. 13 shows that $f(Z)$ is a linear function of Z for the generalized wind profile. Whether the intercept $l_0 = 0.1k(h-d)$, at $Z = 0$ carries any physical meaning is questionable.

4. DISCUSSION

The analysis of windflow above and in the upper levels of an irrigated cotton crop shows that there are strong links between the above- and within-crop microclimates.

In the 3 m above the cotton crop with fetch 150–500 m, the boundary layer was stable for almost the whole day; the degree of stability varied diurnally and with the irrigation cycle. Within the crop there were two distinct regions. In the upper region windspeed profiles were determined by momentum absorption. In the lower region windspeeds were partially determined by large scale pressure gradients and by thermal effects.

In the upper levels of the canopy the assumption of a restricted region of stress divergence led to dimensionless forms for representing a scaleable component of windspeed (Eq. (8)) and the corresponding height (Eq. (7)). From a sample of profiles, representative of a broad range of conditions, the consistency of shape seen in Fig. 10 combined with Eqs. (7) and (8) showed that the dimensionless expressions accurately reflect a scaleable component of the wind. Analysis showed that the diffusivity at the top of the crop corresponded to that predicted from the classical mixing length approach, with the apparent sink of momentum situated at height $z = d + z_0$.

The apparent constancy of the expressions Ψ and $(dU/dZ)_1$ in Eqs. (16) and (17) implies a redundancy of variables, i.e. each expression contains at least one variable dependent on others. Eliminating from these expressions $(dU/dZ)_1$ and $h - z_{\min}$ as dependent variables, leaves $(h-d)$, $(u_h - u_0)$ and u_* as possible independent variables. Detailed examination (not shown) of Figs. 8 and 9 suggests that $(u_h - u_0)$ may be a function of u_* alone with no apparent dependence on $(h-d)$ other than implicit in u_* . Thus it is suggested that the aerodynamic features of the upper levels of the cotton canopy can be scaled by u_* and $(h-d)$ and such scaling factors automatically carry information about crop density and stability as well as windspeed. For example, Fig. 3 implies that $(h-d)$ depends on stability whereas Eqs. (12) and (19) show that momentum diffusivity depends on $(h-d)$ and is apparently independent of stability. This is because $(h-d)$ automatically accounts for the influence of stability on momentum diffusivities within the crop.

A further conclusion is that mixing length, scaled by $(h-d)$ (Eq. (23)), is a dynamic variable tied closely to the above-crop microclimate. The decrease of mixing length with height and the dependence of l on windspeed may be due to changes in the mobility and flexibility of foliage with height.

The similarity between velocity and diffusivity profiles (Figs. 10 and 11) which both show approximately exponential forms, support Cowan's (1968) suggestion that the ratio K_m/u is independent of windspeed.

The aerodynamic features of cotton are therefore consistent with those of other crops, provided account is taken of the relatively dense foliage which restricts the region of stress divergence. The microclimates above and in the upper layers of the canopy are closely linked, and the friction velocity and height of zero-plane displacement play a strong unifying role.

ACKNOWLEDGMENT

This work formed part of a project supported by Ciba-Geigy Ltd.

REFERENCES

- Allan, W. N. and Smith, R. J. 1948 Irrigation in the Sudan in *Agriculture in the Sudan*, (J. D. Tothill, Ed), Oxford University Press, 593-632.
- Bache, D. H. 1975 Transport of aerial spray, III. Influence of microclimate on crop spraying, *Agric. Met.*, **15**, 379-383.
- Bache, D. H. and Uk, S. 1975 Transport of aerial spray, II. Transport within a cotton canopy, *Ibid.*, **15**, 371-377.
- Baines, G. B. K. 1968 A simple heated thermocouple anemometer in *The measurement of environmental factors in terrestrial ecology* (R. M. Wadsworth, Ed). Blackwell Scientific Publications, Oxford, 265-266.
- Bergen, J. D. 1975 An approximate analysis of the momentum balance for the airflow in a pine stand in *Heat and mass transfer in the biosphere*, (D. A. de Vries and N. H. Afgan, Eds). Scripta Book Company, Washington, D.C., 287-298.
- Businger, J. A. 1975 Aerodynamics of vegetated surfaces, in *Heat and mass transfer in the biosphere*, (D. A. de Vries and N. H. Afgan, Eds). Scripta Book Company, Washington, D.C., 139-165.
- Cionco, R. M. 1965 A mathematical model of air flow in a vegetative canopy, *J. Appl. Met.*, **4**, 517-522.
- Cowan, I. R. 1968 Mass, heat and momentum exchange between stands of plants and their atmospheric environment, *Quart. J. R. Met. Soc.*, **94**, 523-544.
- Davenport, D. C. and Hudson, J. P. 1967 Local advection over crops and fallow. I. Changes in evaporation rates along a 17 km transect in the Sudan Gezira, *Agric. Met.*, **4**, 339-352.
- den Hartog, G. and Shaw, R. H. 1975 A field study of atmospheric exchange processes within a vegetative canopy, in *Heat and mass transfer in the biosphere*, (D. A. de Vries and N. H. Afgan, Eds). Scripta Book Company, Washington D.C., 299-309.
- Geiger, R. 1965 *The climate near the ground*, Harvard University Press, Cambridge, Mass.
- Inoue, E. 1963 On the structure of airflow within crop canopies, *J. Met. Soc.*, Japan, Ser. II, **41**, 317-326.
- Ireland, A. W. 1948 The climate in the Sudan, *Agriculture in the Sudan*, (J. D. Tothill, Ed). Oxford University Press, 62-83.
- Isobe, S. 1964 Zero-plane displacement in relation to extinction of momentum flux in crops, *Bull. Natn. Inst. Agric. Sci., Tokyo, Ser. A.*, **11**.
- Monteith, J. L. 1973 *Principles of environmental physics*, Arnold, London.
- Munro, J. M. and Farbrother, H. G. 1969 Composite plant diagrams in cotton, *Cott. Gr. Rev.*, **46**, 261-282.
- Oliver, H. R. 1975 Ventilation in a forest, *Agric. Met.*, **14**, 347-355.
- Rijks, D. A. 1968 Water use by irrigated cotton in Sudan. II. Net radiation and soil heat flux, *J. Appl. Ecol.*, **5**, 685-706.
- 1971 Water use by irrigated cotton in Sudan. III. Bowen ratios and advective energy, *J. App. Ecol.*, **8**, 643-663.
- Saito, T. 1964 On the wind profile within plant communities, *Bull. Natn. Inst. Agric. Sci., Tokyo, Ser. A.* **11**, 67-73.
- Stanhill, G. 1975 Cotton in *Vegetation and the atmosphere* (J. L. Monteith, Ed). Academic Press.
- Stanhill, G. and Fuchs, M. 1968 The climate of a cotton crop: physical characteristics and microclimate relationships, *Agric. Met.*, **5**, 183-202.
- Thom, A. S. 1971 Momentum absorption by vegetation, *Quart. J. R. Met. Soc.*, **97**, 414-428.
- Thompson, B. W. 1965 *The climate of Africa*, Oxford University Press.
- Uchijima, Z. and Wright, J. L. 1964 An experimental study of a flow in a corn-plant layer, *Bull. Inst. Agric. Sci., Tokyo, Ser. A.*, **11**, 19-65.
- Webb, E. K. 1970 Profile relationships: the log-linear range, and extension to strong stability, *Quart. J. R. Met. Soc.*, **96**, 67-90.
- Wright, J. L. and Brown, K. W. 1967 Comparison of momentum and energy balance methods of computing vertical transfer in a crop, *Agron. J.*, **59**, 427-432.